

**A NEW GLOBAL MAP OF MERCURIAN SMOOTH PLAINS.** B. Giuri<sup>1</sup>, H. Hiesinger<sup>1</sup>, C. H. van der Bogert<sup>1</sup>,  
<sup>1</sup>Institut für Planetologie, Westfälische Wilhelms-Universität, Wilhelm-Klemm-Str 10, 48149 Münster, Germany  
[gbarbara@uni-muenster.de](mailto:gbarbara@uni-muenster.de).

**Introduction:** The surface of Mercury exhibits a widespread distribution of smooth plains (SPs) with a clear dichotomy between the northern large-scale provinces and the southern small-scale deposits, covering in total about 27% of the globe [1]. SPs are flat, smooth to gently rolling deposits, that are sparsely cratered with numerous surface features (i.e., wrinkle ridges) and have sharp contacts with adjacent terrains [2-3]. From Mariner 10 images, the absence of recognisable volcanic features like domes or vents, and morphological similarities with lunar maria, caused some researchers [4-6] to argue for a volcanic origin for all SPs, while others [7-8] supported an origin via the ballistic emplacement of Caloris ejecta, analogous to lunar light plains, and argued that at least some SPs are not volcanic. However, as arguments for a single impact ejecta origin began to lose momentum among the scientific community, a third hypothesis was proposed that considered impact-triggered volcanism to explain the global distribution of SPs [9], despite the possibility of at least some plains having a mass wasting and/or impact origin [10-11]. Finally, with the MESSENGER mission, evidence supporting widespread effusive and pyroclastic volcanism was finally observed. The high-resolution images obtained and near global coverage of the planet allowed global mosaics, DEMs, and spectral color maps to be computed for regional to global surveys [12], greatly enhancing our understanding of the stratigraphy, geology, and volcanic history of the innermost planet. However, despite numerous studies investigating SPs and the growing consensus for a volcanic origin for most SPs, the origin for some deposits without obvious volcanic features remains debated. In this work, we used high-resolution images from the Mercury Dual Imaging System (MDIS), in combination with other data sets, to study SPs in detail with particular focus on previously unmapped small-scale deposits and crater floors down to 20 km in diameter. Thus, we present a new and independent global map of smooth plains.

**Data and Methods:** In this study, we used the global mosaic basemap (MDIS, 166 m/p) for manually mapping SPs in ArcGIS 10.5 at a scale of 1:1.25 M. The latest regional geologic maps from PlanMap were consulted in the construction of our map [16-19]. SPs

were identified visually based on flatness, smoothness, sharpness of contact with adjacent terrains, and low crater density as per definition by [2]. We aim to integrate our map with roughness maps and the Northern SP (NSP) map from [13] to determine the relative smoothness/roughness of individual plain units to improve the accuracy of our new global map.

**Mapping approach:** The mapping was done via visual identification of flat and smooth deposits that contrast to adjacent intermediate and intercrater terrains (Fig. 1). Unit boundaries are defined by the continuity and sharpness between smooth and more rugged terrain alone. This approach differs from the work of [1], who aimed to map the original extent of a plain regardless of subsequent modification. Thus, if a crater impacted along the plains boundary, we excluded it from the plains unit, i.e., Raditladi basin. However, if a crater impacted within a plain leaving the border uninterrupted, we included it in the overall unit. We also separately mapped ‘possible smooth plains’ (PSP) deposits for which a classification is ambiguous. Due to the large heterogeneity of plains units within craters, we classified their occurrences on floors based on morphology, similarity to NSPs or adjacent SP unit, embayment and visibility of impact structures like peaks, rings etc. down to 20km in diameter as: 1) smooth crater floors ‘c’ (scf\_c) which are ghost-like craters, almost or completely filled by SP, often found around large-scale deposits and with no visible impact structures, such as rings or peaks; 2) smooth crater floors 1 (scf\_1) which are craters with visible peaks, remnants of a ring structure and terraces, with the floor or fill resembling SP-like deposits of uncertain composition; and 3) smooth crater floors (scf) which represent the rest of craters with a smooth and flat floor with a uncertain origin. We also classified a fourth type of crater floor, called IM (impact melts), morphologically different from the previous classes, brighter and often exhibiting hollows.

**Results and Discussion:** In our new map, we find that large-scale deposits like the NSP, in Caloris, and in areas around the Caloris basin are generally similar to earlier maps [1-2;14]. Small scale deposits, some previously unmapped, appear sparse and globally distributed – mostly within crater floors and of higher

density compared to previous work [1-2;14-15]. In particular, the differences reflect: 1) the different mapping technique; and 2) the mapping of isolated and crater floor deposits down to 20 km. Despite the uncertainty for crater floors smaller than 100 km as inferred by [1], we aimed at mapping all identifiable smooth and flat deposits regardless of their origin, which includes crater floors down to a size for which ghost craters are recognisable and mappable. The new more detailed map, based on the most recent geologic maps, provides a more complete depiction of the global distribution of SPs. This map also provides a basis for examining alternative hypotheses for deposits of uncertain origin, including emplacement as: 1) distal impact ejecta; 2) proximal impact material or impact melt deposits; or 3) a combination of all of the above.

We find that the SPs in our new map, including scf\_c, cover about 33.5% of the globe, slightly more than found by [15]. Finally, we identified several large flat areas, for example around Praxiteles basin, Wang Meng, N and W Sihtu Planitia, Renoir basin, between Hemingway and Warhol basins, around Vieira de Silva and Jokai, where the surface appears fractured, cratered, and knobby, as well as smooth in places, but with no clear contacts, hence some SPs deposits in these regions might have been missed. It is therefore possible that SPs cover an even greater surface area than indicated by our map. Nevertheless, the mapping of isolated deposits including crater floors provides the first near complete map of smooth deposits on Mercury.

**Conclusion and Future Work:** Our new map of SPs occupy 33% of the surface of Mercury, showing similarities with prior maps. However, we find a higher density of small-scale isolated deposits spread around the globe and within craters down to 20 km in diameter, increasing of 6% the global surface area distribution of SPs. We separated crater floors into three morphological classes, with a fourth class for craters containing hollows. We also identified large intermediate flat regions with SP-like appearance perhaps indicative of separate SP emplacement events. It is likely that the true extent of SPs is greater than previously mapped, including in this work. We are now in the process of finalising our study by consulting roughness maps for available quadrangles in order to improve the completeness of our map even further.

**REFERENCES** : [1] Denevi, B. W. et al. (2013). *J. Geophys. Res. Planets*, 118, 891-907; [2] Trask & Guest (1975). *J. Geophys.*

*Res.*, 80, 2461-2477; [3] Spudis & Guest (1988). *Mercury*, edited version, pp. 118-164; [4] Murray, B. C. et al. (1975). *J. Geophys. Res.* 80, 2508-2514; [5] Strom, R. G., et al. (1975). *The geo. Of Terr. Planets*, pp. 13-55, NASA SP 469; [6] Trask & Strom (1976). *Icarus* 28, 559-563; [7] Wilhelms, D- E., (1976). *Icarus* 28, 551-558; [8] Oberbeck, V. R. et al., (1977). *J. Geophys. Res.* 82, 1681-1698; [9] Kiefer & Murray (1987). *Icarus* 72, 477-491; [10] Watkins, J. A., (1980). *Reports of Plan. Geo. Program*, pp. 37-39, NASA TM 81776; [11] Spudis & Guest, (1987). *Mercury*. Univ. of Arizona Press, Tucson, in press.; [12] Byrne, P. K., (2018). Cambridge University Press, 2018, pp. 287-323; [13] Kreslavski, M. A. et al., (2014). *Geophys. Res Lett.*, 41, 8245-8251 ; [14] Prockter, L. M., et al. (2016). 47<sup>th</sup> LPSC abstract 1245 ; [15] Wang, Y., et al., (2021). *Geophys. Res. Letters*, 48 ; [16] Galluzzi, V., et al., (2016). H02. *Journal of Maps*; [17] Wright, J., et al., (2020). H05. *PlanMap*; [18] Malliband, C. C., et al., (2020). H10. *PlanMap*; [19] Pegg, D. L., et al., (2020). H14. *PlanMap*.

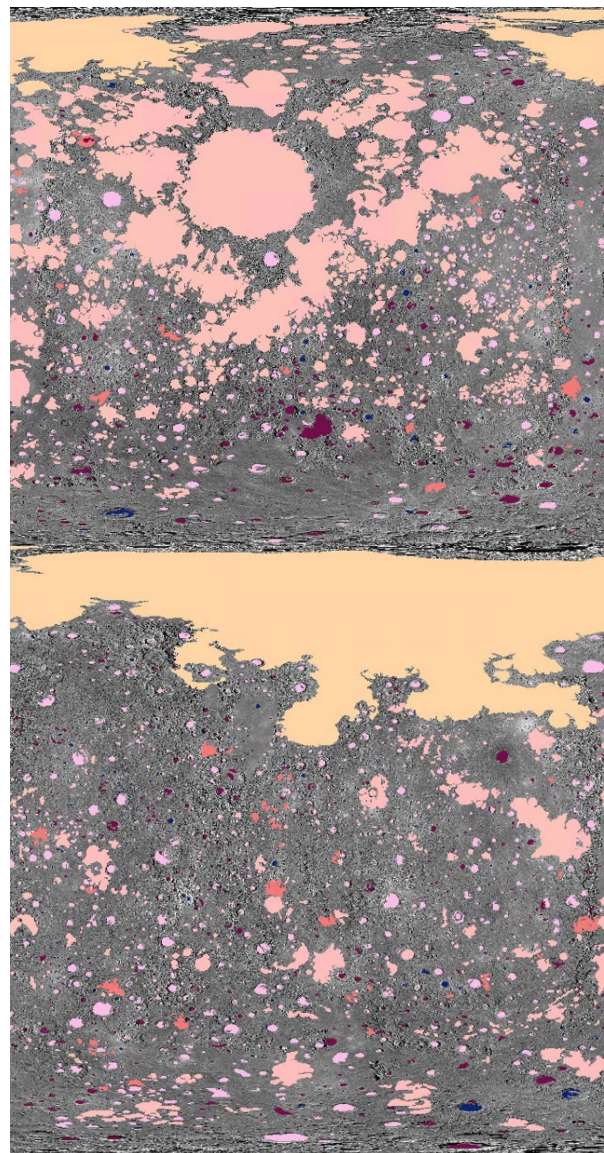


Fig 1: Top image: Caloris centred map and bottom image: Caloris antipode. SPs in coral pink, NSP in beige; PSPs in coral red; IM in navy blue; scf\_1 in lilac and scf in purple.